Journal of Fluorine Chemistry 135 (2012) 330–338

Contents lists available at SciVerse ScienceDirect

Journal of Fluorine Chemistry

journal homepage: www.elsevier.com/locate/fluor

Amino-ethoxilated fluorinated amphiphile: Synthesis, self-assembling properties and interactions with *ss*DNA

Nicolas Dupuy [a], Andreea Pasc [a,1,*], Stéphane Parant [b], Stéphane Fontanay [c], Raphaël E. Duval [c], Christine Gérardin [a]

[a] *LERMAB – EA 4370, Nancy-Université, BP 70239, F-54506 Vandoeuvre-lès-Nancy, France*
[b] *UMR 7565 SRSMC, Nancy-Université, BP 70239, 54506 Vandoeuvre-lès-Nancy, France*
[c] *GEVSM, SRSMC, UMR UHP-CNRS 7565, Nancy-Université, Faculté de Pharmacie, 5 rue A. Lebrun, B.P. 80403, 54001 Nancy Cedex, France*

ARTICLE INFO

Article history:
Received 8 November 2011
Received in revised form 28 December 2011
Accepted 29 December 2011
Available online 8 January 2012

Keywords:
Vesicles
Fluorinated surfactant
*ss*DNA-nanovectors

ABSTRACT

Fluorinated compounds are not only more hydrophobic than their hydrogenated counterparts but also oleophobic. This makes them interesting for biomedical applications. They form a large variety of supramolecular architectures and, if appropriately designed, they spontaneously form vesicles. Herein we report the synthesis of novel monocatenar fluorinated surfactant, named **$F_9NH(EO)_2NH_2$**, its use as *ss*DNA vector with potential applications in gene delivery or RNA interference. The molecular structure of the amphiphilic compound was designed in three parts: (i) *a fluorinated hydrophobic tag* responsible of self-assembling, (ii) a flexible and hydrophilic *ethylenoxide moiety* as polar head and (iii) *a protonated* at physiological pH *primary amine* responsible of binding. Surface tension, dynamic light scattering (DLS) measurements, and TEM studies showed that the monocatenar surfactant **$F_9NH(EO)_2NH_2$** spontaneously self-assembles into vesicles. This represents another example in addition to the few existing in the literature and it highlights the unique properties of the fluorinated tail. Interactions between *ss*DNA and cationic monocharged **$F_9NH(EO)_2NH_2$** were probed by static light scattering (SLS), fluorescence and circular dichroism (CD). **$F_9NH(EO)_2NH_2$** was found to exclude ethidium bromide (EB) from *ss*DNA/EB complex, and this process was dependent on the *ss*DNA concentration and on the charge ratio surfactant to *ss*DNA. CD spectra showed that by increasing the surfactant concentration, *ss*DNA undergoes a continuous conformational transition from native B-form to a more ordered phase ($Z_+/Z_- \leq 3$) and then to a less ordered phase ($Z_+/Z_- \geq 4$), which confirmed the results obtained by fluorimetry and SLS measurements. Cell viability studies reveled that monocatenar fluorinated surfactant **$F_9NH(EO)_2NH_2$** is not toxic for human cells (MRC-5) below 40 μM.

1. Introduction

With the development of vector-mediated drug or gene delivery, scientific attention is continuously shifting toward "smart" supramolecular architectures with refined, multiple functions. Among these, the most commonly used nanovectors are liposomes. They serve as convenient delivery vehicles for biologically active molecules or genetic material. Lipid-drug aggregates are easy to form and sensitive to structural manipulations, allowing adjustments of their properties in pursue of particular purposes. Both liposomes, obtained from natural phospholipids, and vesicles, made from synthetic amphiphiles, have a wide range of applicability, and have become very promising forms of molecular medicine.

Encapsulation of nucleotidic fragments (DNA or RNA) is of particular interest in gene therapy [1–4] or RNA interference [5]. To do so, synthetic systems based on various lipids (*e.g.* lipoplexes) have been developed with the aim to protect the nucleic acids from degradation, to increase their circulation life time and the possibility to achieve partially or totally targeted gene delivery [6–8].

Cationic liposomes [9–14] have been suggested as possible agents for non-viral gene delivery since they offer several advantages: (i) positively charged interfaces which can efficiently complex *ss*DNA through electrostatic interactions, (ii) due to their membranous nature, they can assist the delivery of *ss*DNA inside the cells. However, when designing novel vectors for nucleic acids one should take into account not only the hydrophilic part, usually responsible for the *ss*DNA complexation, but also the hydrophobic domain [15] responsible for the physical features of the bilayer (*i.e.* phase transition temperature, fluidity) and influencing the stability of the lipoplexes. From this point of view, fluorinated surfactants are of particular interest and many cationic fluorinated

* Corresponding author. Tel.: +33 0383 684 344; fax: +33 0383 684 322.
E-mail address: andreea.pasc@srsmc.uhp-nancy.fr (A. Pasc).
[1] Current address: UMR 7565 SRSMC, Nancy-Université, BP 70239, 54506 Vandoeuvre-lès-Nancy, France.

0022-1139/$ – see front matter © 2012 Elsevier B.V. All rights reserved.
doi:10.1016/j.jfluchem.2011.12.017

amphiphiles have been developed as transfecting agents [16–23]. It was suggested that the enhanced transfection efficiency was related to the fluorous tags, more hydrophobic and more lipophobic and therefore less damaged by biomolecules *in vivo*. Fluorinated vesicles are more stables than hydrogenated ones and are less recognizable by macrophages [21,24]. Moreover, the biophysical behavior of these compounds seems to be related not only to the presence of the fluorinated domain in the molecule but also to its position with respect to the hydrophilic part [25].

Our group previously reported the synthesis of fluorinated compounds bearing two hydrophobic chains and their interactions with *ss*DNA in monomolecular film [26]. We have now investigated the synthesis and self-assembly properties of a monocatenar surfactant consisting of (i) *a fluorinated hydrophobic tag* responsible of self-assembling, (ii) *an ethylenoxide moiety* sufficiently hydrophilic avoid precipitation of the surfactant–*ss*DNA complex and (iii) *a protonated* at physiological pH *primary amine* responsible of binding. Our goal was to obtain a high water-soluble surfactant spontaneously forming vesicles entrapping drug or gene carriers. Herein, we describe the physico-chemical properties of this fluorinated surfactant, including its interaction modes with *ss*DNA. A preliminary assessment of its toxicity properties is also presented.

2. Experimental

2.1. Materials

All solvents were reagent grade unless otherwise specified and used without further purification. Starting fluorinated alcohols were purchased from Dupont (see Scheme 1 and Ref. [29]). NMR spectra were recorded on a Bruker AM 400 or an AC 200 instrument. Chemical shifts are reported in ppm relative to TMS as internal standard for the ^{1}H spectra and to $CFCl_3$ for the ^{19}F spectra. Melting points were determined using a Kofler bank and were not corrected. IR spectra were recorded on a Perkin-Elmer FTIR "spectrum one" in ATR mode. Ultrapure water (Elix 3 Millipore, surface tension of 72.5 mN m^{-1} at 20 °C, resistivity of at least 15 MΩ cm) was used for surfactant solutions. *ss*DNA (M = 7404 Da, AAC-TCG-GAA-TGG-AGA-ACA-CAG-ATC) was purchased from Eurogentec. MRC-5 cells (human pulmonary embryonic fibroblasts, ATCC CCL-171) were obtained from BioMerieux (France).

2.2. Synthesis

2.2.1. 3-{2-[2-(2-Amino-ethoxy)-ethoxy]-ethylamino}-4,4,5,5,6,6,7,7,8,8,9,9,10,10,11,11,12,12,12-nonadecafluoro-dodec-2-enoic acid ethyl ester, $F_9NH(EO)_2NH_2$ enamine

A mixture of 1 eq. of ethyl 3-perfluorononyl-3-fluoropropenoate, 10 eq. of 2-[2-(2-amino-ethoxy)-ethoxy]-ethylamine and 30 eq. Et_3N in 100 mL Et_2O was heated to reflux for 24 h. Et_2O and Et_3N were then removed under vacuum and the resulting mixture was re-dissolved in ether and washed with 3 × 100 mL water. The organic phase was dried on $MgSO_4$ and the solvent evaporated. The final product was purified on silica gel (hexane/AcOEt, 9:1) or recrystallized in hexane. Yield 90%, viscous oil, IR (KBr) 3357, 3265, 1671, 1622, 1300–1100 cm^{-1}; ^{1}H NMR ($CDCl_3$): δ 8.62 (s, 1H, NH), 5.03 (s, 1H, Z C<u>H</u>=); 4.15 (q, 2H, CH_2OCO, $^3J_{HH}$ = 6 Hz); 3.45–3.67 (m, 10H, O<u>CH$_2$C</u><u>H$_2$</u>O, C<u>H$_2$C</u><u>H$_2$</u>NH, C<u>H$_2$</u>CH$_2$NH$_2$); 2.88 (s, 2H, CH$_2$C<u>H$_2$</u>NH$_2$); 1.71 (m, 2H, NH_2); 1.27 (t, 3H, CH_3, $^3J_{HH}$ = 6 Hz); ^{13}C NMR ($CDCl_3$): δ 169.00 (COO); 147.82 (C=); 106–120 (m, CF_2 and CF_3); 96.23 (<u>C</u>H=); 73.08 (O<u>C</u>H$_2$<u>C</u>H$_2$O); 70.77 (<u>C</u>H$_2$CH$_2$NH); 60.32 (<u>C</u>H$_2$CH$_2$NH$_2$); 53.19 (<u>C</u>H$_2$OCO); 44.73 (CH$_2$<u>C</u>H$_2$NH); 41.75 (CH$_2$<u>C</u>H$_2$NH$_2$); 13.42 (CH_3); ^{19}F NMR ($CDCl_3$): δ −81.23 (s, CF_3); −111.33 (m, CF_2C=); −121.89 to −126.61 (m, CF_2). $C_{20}H_{21}F_{19}N_2O_4$: calcd. C 33.61, H 2.94, N 3.92, found C 32.99, H 2.44, N 3.51.

2.2.2. 3-{2-[2-(2-Amino-ethoxy)-ethoxy]-ethylamino}-4,4,5,5,6,6,7,7,8,8,9,9,10,10,11,11,12,12,12-nonadecafluoro-dodecanoic acid ethyl ester, $F_9NH(EO)_2NH_2$

1 Eq. of enamine dissolved in 50 mL AcOEt/20 mL MeOH and catalytic amount of Ni Raney were introduced in a hydrogenation reactor working under 80 bar H_2. After 24 h at 50 °C, the mixture was cooled down to room temperature, purged with N_2 and filtered on celite. The solvent was then removed under vacuum and the resulting product was re-dissolved in AcOEt and dried on $MgSO_4$. The final product was recovered after evaporation of the solvent, without further purification. Yield 87%, viscous oil. IR (KBr) 3366, 1739, 1300–1100 cm^{-1}; ^{1}H NMR ($CDCl_3$): δ 4.18 (q, 2H, CH_2OCO, $^3J_{HH}$ = 7.5 Hz); 3.83 (m, 1H, C<u>H</u>NH); 3.51–3.59 (m, 8H, O<u>CH$_2$C</u><u>H$_2$</u>O, C<u>H$_2$</u>CH$_2$NH$_2$, C<u>H$_2$</u>CH$_2$NH); 2.77–2.90 (m, 4H, CH$_2$C<u>H$_2$</u>NH, CH$_2$C<u>H$_2$</u>NH$_2$); 2.58–2.76 (m, 2H, CHC<u>H$_2$</u>); 1.98 (m, 3H, NH, NH_2); 1.27 (t, 3H, CH_3, $^3J_{HH}$ = 7.5 Hz); ^{13}C NMR ($CDCl_3$): δ 170.44 (COO); 106–120 (m, CF_2 and CF_3); 70.99 (O<u>C</u>H$_2$<u>C</u>H$_2$O); 70.33 (<u>C</u>H$_2$CH$_2$NH); 61.18 (<u>C</u>H$_2$CH$_2$NH$_2$); 56.30 (<u>C</u>H$_2$OCO, CH); 47.09 (CH$_2$<u>C</u>H$_2$NH); 41.71 (CH$_2$<u>C</u>H$_2$NH$_2$); 14.17 (CH_3); ^{19}F NMR ($CDCl_3$): δ −81.23 (s, CF_3); −115 to −117 (m, CF_2CHNH); −121.89 to −126.61 (m, CF_2). $C_{20}H_{23}F_{19}N_2O_4$: cacld. C 33.51, H 3.21, N 3.91, found C 33.41, H 3.09, N 3.72.

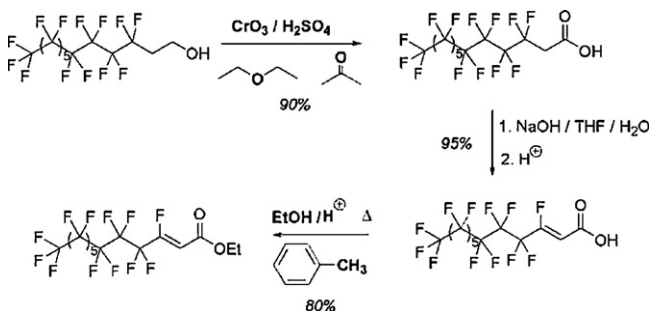

Scheme 1. Synthesis of ethyl 3-perfluorononyl-3-fluoropropenoate.

2.3. Surface tension measurements

Surface tension (γ) measurements were carried out with a Digital Tensiometer KRUSS K10ST using the Wilhelmy method. Surfactant solutions were prepared in pure water or in phosphate buffered solution (pH = 7.4). All the measures were carried out at 20 °C.

2.4. Light scattering measurements

The measurement of the particle size and polydispersity were performed by dynamic light scattering experiments, using a Zetasizer 3000 Has (Malvern Instruments Ltd.) with a light source He–Ne laser (wavelength 633 nm). The scattering angle was 90°. All solutions were filtered in nanopure water or in buffer solution before any measurement (filter 450 nm) and all the measures were carried out at 20 °C. The determinations of the CAC (critical aggregation concentration) were carried out by Static light scattering (SLS) at 20 °C using a fluorospectrometer, model Fluorolog 3 Jobin Yvon in time-drive mode with quartz cell with a section of 1 cm × 1 cm. Incident light of 633 nm was used and the scattered light was also collected at 600 nm at the scattering angle of 90° during 300 s (increment time 1 s). The minimum intensity of the scattered light was recorded for each concentration. All the solutions were prepared in pure water or in phosphate buffered solution (pH 7.4).

2.5. Transmission electron microscopy

TEM studies were performed using a Philips CM20 type microscope at 200 keV. Samples for TEM were prepared by the negative-staining technique with a 2% sodium phosphotungstate solution buffered at pH 7.5. A drop of sample solution was left on the carbon-coated copper grids for 1 min, then the excess liquid was removed and the contrasting agent was deposited.

2.6. Fluorimetry: ethidium bromide displacement assay

EB intercalation between bases was determined through fluorescence spectroscopy using a fluorospectrometer, model Fluorolog 3 Jobin Yvon with quartz cell with a section of 1 cm × 1 cm (excitation of 270 nm, emission of 610 nm). The *ss*DNA was mixed with EB solution (1 EB per base) and then the cationic amphiphile solution in phosphate buffer (TRIS 0.05 M, NaCl 0.15 M, pH = 7.4) was added in order to obtain amphiphile/*ss*DNA complexes at Z_+/Z_- molar ratios varying from 0 to 8 (0.1 μM *ss*DNA/2.5 μM EB, 0.3 μM *ss*DNA/7 μM EB and 2.5 μM *ss*DNA/60 μM EB, titration surfactant concentration was 3.5 mM). The samples were mixed gently and the fluorescence was measured at room temperature after 20 min.

2.7. Circular dichroism

Circular dichroism was performed at 20 °C on a MOS450 spectropolarimeter (Bio-Logic) using 1 cm path length quartz cells in the range 210–320 nm at 4 nm band with 0.5 nm step size and 2 s time per point. CD titration was performed with at a fixed *ss*DNA concentration: 2 μM in a phosphate buffer solution (NaCl 0.15 M, TRIS 0.05 M and pH 7.4) and various concentrations of amphiphiles.

2.8. Biological studies: Cell line, cell culture

Freshly trypsinized MRC-5 cells (human embryonic lung fibroblasts, ATCC CCL-171) were seeded at 1×10^5 cells cm^{-2} and grown in minimum essential medium (MEM, 41090, Invitrogen, France), supplemented with 10% decomplemented fetal calf serum (FCS, 10270, Lot 40Q5150 K, Invitrogen, France). Cultures were maintained in a humidified atmosphere with 5% CO_2 at 37 °C. Cell viability was determined by the trypan blue dye exclusion method. For all experiments, cells were allowed to adhere and grow for 48 h in culture medium prior to exposure to **$F_9NH(EO)_2NH_2$**.

2.9. MTT assay

To evaluate the effect of **$F_9NH(EO)_2NH_2$** on MRC-5 cells, the MTT colorimetric assay was performed as described in Refs. [27,28]. This test is based upon the selective ability of living cells to reduce the yellow salt MTT [3-(4,5-dimethyl-2-thiazolyl)-2,5-diphenyl-2H-tetrazolium bromide] (MTT, 135038, Aldrich, France), to a purple-blue insoluble formazan precipitate. Experiments were performed in 100 μL of medium in flat-bottom 96-well plates (Sarstedt, France). After 48 h incubation of MRC-5 cells at an initial density of 1×10^4 cells per well, the medium was removed and replaced by 2% decomplemented FCS medium containing **$F_9NH(EO)_2NH_2$** (5×10^{-4} to 1×10^{-12} M). After each period of incubation (24 h, 48 h and 168 h), stock MTT solution (5 mg mL^{-1} MTT in phosphate buffered saline (PBS)) was added (10 μL per 100 μL medium) and plates were incubated in a humidified atmosphere with 5% CO_2 at 37 °C for 4 h. Then 100 μL sodium dodecyl sulfate (SDS, L-5750, Sigma, France) (0.1 g mL^{-1} SDSin PBS, with 445 μL HCl 0.01 M) were added to each well, in a humidified atmosphere with 5% CO_2 at 37 °C for 4 h more. The amount of formazan formed was obtained by scanning with an ELISA reader (Titertek Multiscan MCC/340 MK II apparatus, Labsystems, Helsinki, Finland) at a wavelength of 540 nm with reference at 690 nm. Height wells per dose and time point were counted in three different experiments.

3. Results and discussion

3.1. Synthesis of fluorinated surfactants

The molecular structure of the surfactant **$F_9NH(EO)_2NH_2$** was designed in three parts: (i) *a fluorinated hydrophobic tag* responsible of self-assembling, (ii) *a* flexible and hydrophilic *ethylene oxide moiety* as polar head and (iii) *a protonated* at physiological pH *primary amine* responsible of binding.

The starting dehydrofluorinated esters were prepared by Fischer esterification of dehydrofluorinated acids (Scheme 1), which were prepared as previously reported by our group, from commercially available perfluorodecylethanol (1H,1H,2H,2H-2-perfluorododecanol), by oxidation with chromic acid and deshydrofluoration with aqueous NaOH [29].

We had previously shown that unsaturated esters of this type can react with different oxygenated nucleophiles to give ketals or enol-ethers by a Michael addition mechanism and fluorine elimination [30]. They are also able to react with nucleophile-like azide or amines and this leads to enamines [31–33].

The amphiphile reported in this paper ensued from the reaction between ethyl-3-perfluorononyl-3-fluoropropenoate and 2-[2-(2-aminoethoxy)-ethoxy] ethylamine (Scheme 2). The addition of the diamine to the double bond and the elimination of the fluorine gave the corresponding **$F_9NH(EO)_2NH_2$** enamine, which was then hydrogenated under relatively hard conditions (80 bar, 80 °C), and Raney Nickel as a catalyst. The desired fluorinated surfactant **$F_9NH(EO)_2NH_2$** was obtained with relatively good overall yield (60%).

3.2. Amphiphilic properties

Surface tension measurements of **$F_9NH(EO)_2NH_2$** were performed in pure water and in buffered solutions, close to the physiological conditions at pH 7.4 (Fig. 1). Moreover, surface

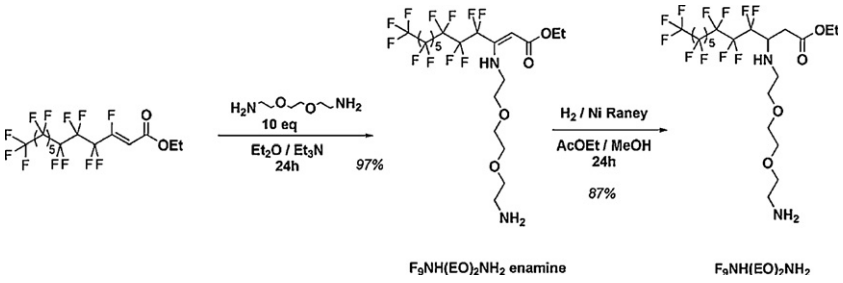

Scheme 2. Synthesis of fluorinated surfactant **$F_9NH(EO)_2NH_2$**.

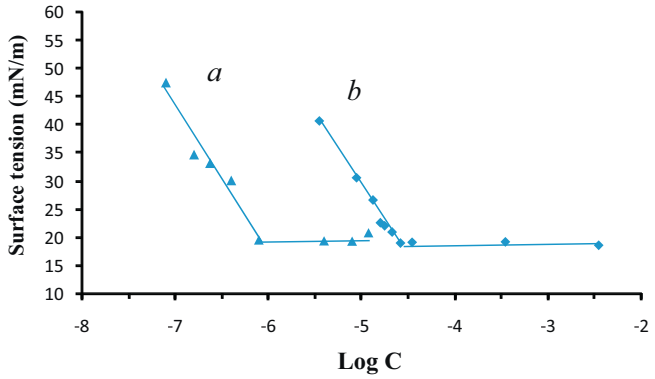

Fig. 1. Variation of the surface tension (mN m^{-1}) as a function of log of concentration (mol L^{-1}) of **$F_9NH(EO)_2NH_2$** (a) in pure water and (b) in buffer phosphate (NaCl 0.15 M, TRIS 0.05 M, pH 7.4).

tension measurements allowed us to estimate the molecular area at the interface, from the inverse of the surface excess concentration (Γ) calculated according to the Gibbs equation (Table 1). The minimal values of the surface tension and the CAC, as well as the estimated main area per molecule (A) of the absorbed cationic surfactant are shown in Table 1.

In both media, the minimal surface tension reached a plateau at 19 mN m^{-1}, whereas the CAC value of the surfactant was 10 times higher in buffered solution than pure water. At this pH, the compound is cationic (the primary amine is protonated). Usually, the addition of salt compresses the double electric layer of the polar head of ionic surfactants. This can produce a screening of the electrostatic repulsions between neighboring hydrophilic groups and, therefore, enables the aggregation to a lower surfactant concentration. However, in our case, the addition of salt increases the CAC. The same effect has been observed with anionic surfactant [34].

The estimated molecular area in buffered and pure water, 37 and 36 Å^2, respectively are higher than the cross sectional area of the fluoroalkyl chain (27–30 Å^2). Thus, the molecular area at the interface seems to be governed by both contributions of fluorinated and ethylene oxide segments, which are slightly tilted with respect to the normal at the interface (Fig. 2). This might be due (i) to the stiffness of the fluorinated chain and the absence of the any "gauche" defects and (ii) to the intramolecular hydrogen-bonding between the internal amine and the ester group (N–H···O=C).

$F_9NH(EO)_2NH_2$ has two pH sensitive amine moieties. Estimated pK_a values[2] are 8.7 for NH_2 and 3.8 for NH, respectively, indicating thus that, at physiological pH, only the primary amine is protonated. This is particularly important since the external binding amine group has to be protonated in physiological conditions in order to interact with *ss*DNA. These pK_a values take into account the electronic effects of the fluorinated chain and the ester group which stabilizes the NH form in the β position of the fluorinated segment. Moreover, this form is stabilized par intramolecular H-bonding.

In the Gibbs equation for ionic surfactants, one should consider the $(z+1)$ factor

$$\Gamma = -\frac{1}{2.3RT}\frac{d\varphi}{d\log c}(z+1)$$

where z is the charge of the surfactant, to take into account the associated counter ions and Γ is the surface excess concentration. Also in buffered solutions, $z = 1$, as the salt concentration exceed

[2] ACD/pK_a, Advanced Chemistry Development, Inc., Toronto, ON, Canada, www.acdlabs.com.

Table 1
Amphiphilic values of **$F_9NH(EO)_2NH_2$** in water and phosphate buffer as determined by (A) surface tension and (B) SLS measurements.

Subphase	A/molecule (Å^2)	Δ (mN m^{-1})	CAC (mol L^{-1})	
Pure water	37	19	(A) 8×10^{-7}	(B) 4×10^{-6}
Phosphate buffer	36	19	(A) 2×10^{-5}	(B) 1×10^{-5}

the surfactant concentration, and therefore salt is screening the partial charges of the surfactant. As the estimated molecular area are almost identical in buffered or pure water solutions, one can conclude that **$F_9NH(EO)_2NH_2$** has only one charge, which confirms that only the primary amine is protonated at this pH.

DLS measurements were carried out on 1 mM dispersions of **$F_9NH(EO)_2NH_2$** in pure water and in buffer phosphate and the hydrodynamic size and the polydispersity of the aggregates were determined. The measurements show two populations, centered 50 nm and 300 nm, and these aggregates were stable at room temperature for at least 48 h. Above CAC, the size of the vesicles did not changed with the dilution. Moreover, TEM micrographs allow us to visualize these aggregates (see insets *a* and *b* in Fig. 3).

Thus, **$F_9NH(EO)_2NH_2$** has the ability to spontaneously self-assemble into vesicles in aqueous solutions, which is rare for monocatenar surfactants. Indeed, to date, only a few examples of this kind are known [18,35–38]. This phenomenon seems to be related to the particular features of fluorinated chains and to the asymmetry of the molecule [39]. The relatively large size of these aggregates let us imagine their usage for the encapsulation of the *ss*DNA. To do so, surfactant solutions of **$F_9NH(EO)_2NH_2$** were mixed with different ratio of *ss*DNA and SLS, fluorimetry and circular dichroism measurements were carried out in order to investigate *ss*DNA/surfactant interactions.

SLS measurements can punctually be used for CAC determination [40] and are commonly interpreted within the RGD approximation (Rayleigh–Gans–Debye). This approximation depends on two assumptions about the properties of vesicles: (i) that the index of refraction (n_1) of the vesicle is close to that of the medium (herein water, n_0) and (ii) that the size of the vesicle (a) is smaller than the instrumental light wavelength used (λ). These conditions are often expressed using the following two inequalities:

$$\left|\frac{n_1}{n_0}-1\right| \ll 1 \quad (1)$$

$$\frac{4\pi a}{\lambda} < 1 \quad (2)$$

In our case, both conditions are respected: (i) fluorinated compounds have one of the lowest index of refraction (*i.e.* 1.33 for perfluorohexane) and (ii) the size of the vesicles, as determined by DLS, is smaller than the incident light wavelength of our instrument, λ = 633 nm.

SLS measurements were carried out with different concentrations of **$F_9NH(EO)_2NH_2$** in water and in buffer solutions (Fig. 4) and the results are showed in Table 1. The inflection on the curves corresponds to the CAC values and they are in the same range of values as those obtained by tensiometry (Fig. 1, Table 1).

This technique has significant advantages: rapidity, small quantity of product and precision of measurements. This is why, it appeared interesting to us to use this technique to study the interactions between the fluorinated surfactant and *ss*DNA.

SLS measurements of *ss*DNA/**$F_9NH(EO)_2NH_2$** mixtures were carried out in buffer solutions at a given *ss*DNA concentrations and various surfactant concentrations. In the first case, the [*ss*DNA] was fixed at 10^{-7} M and in the second case [*ss*DNA] = 2×10^{-6} M. Plots of scattered light intensity *vs.* surfactant concentration, presented

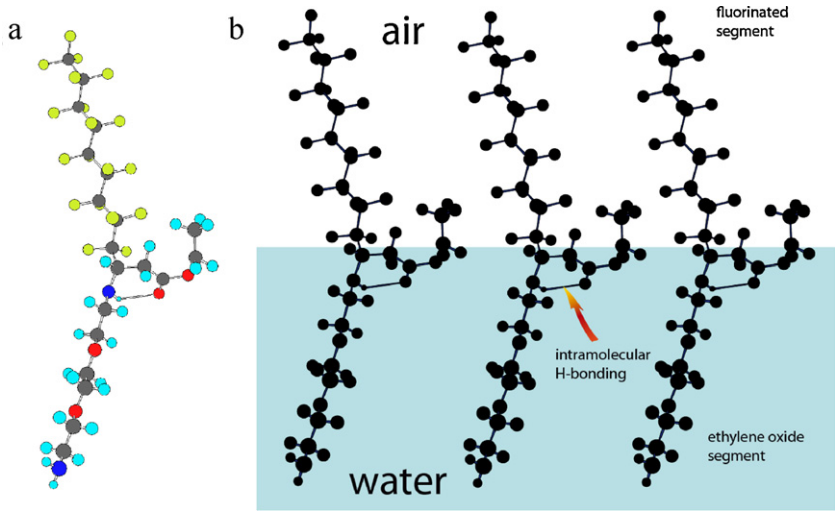

Fig. 2. (a) Molecular modeling of $F_9NH(EO)_2NH_2$ as determined with MOPAC method, CS Chem Office (b) suggested self-assembled Gibbs layer of $F_9NH(EO)_2NH_2$.

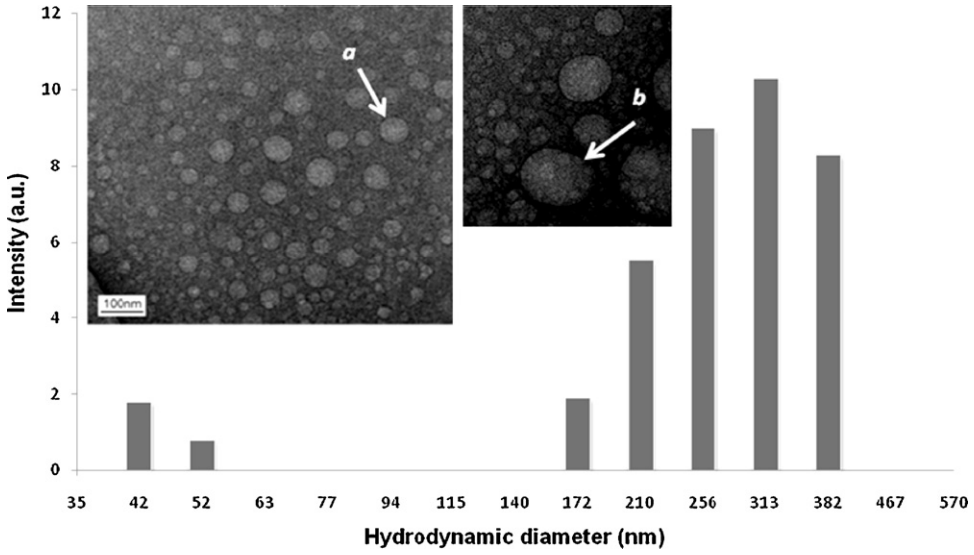

Fig. 3. DLS measurements of 1 mM dispersion of $F_9NH(EO)_2NH_2$ in buffer phosphate show two populations of aggregates centered on 50 nm and 300 nm. Insets (a) and (b) correspond to the TEM micrographs of $F_9NH(EO)_2NH_2$ in buffer phosphate and its show vesicles of 50 and 100 nm (on both insets, 1 cm corresponds to 100 nm).

in Fig. 5 top, show several inflections indicative of diverse interaction modes between $F_9NH(EO)_2NH_2$ and *ss*DNA.

At low concentration, the surfactant is in a monomeric form and *ss*DNA/$F_9NH(EO)_2NH_2$ interactions are weak (Fig. 5 bottom, region a of the schematic curve and inset a). When the surfactant concentration increases, (b) micellization of the surfactant on the *ss*DNA matrix occurs [41–43]. The inflection point at this level corresponds to the critical aggregation concentration of the surfactant onto the *ss*DNA matrix allowing the formation of micelles (CACmDNA). A plateau is then reached (c) corresponding to the maximum number of surfactant molecules which are able to micellize onto *ss*DNA. If the concentration in surfactant is still

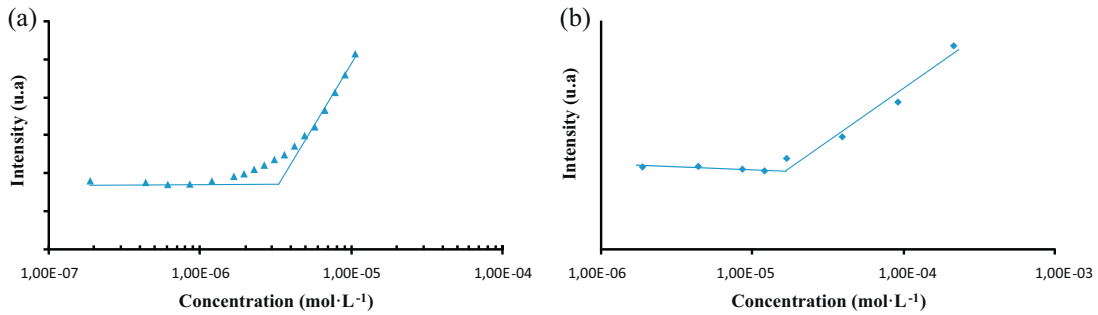

Fig. 4. Static light scattering of $F_9NH(EO)_2NH_2$ (a) in pure water and (b) in buffer phosphate (NaCl 0.15 M, TRIS 0.05 M, pH 7.4).

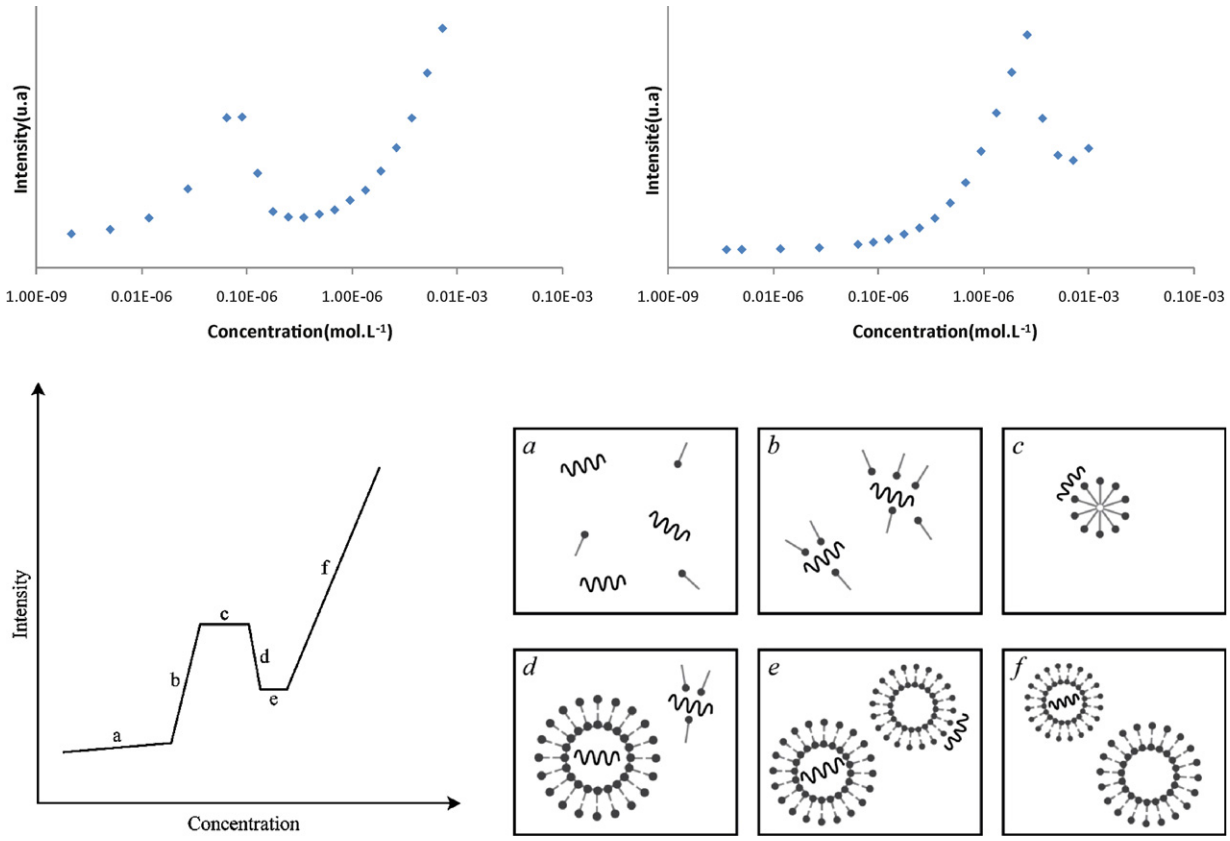

Fig. 5. *ss*DNA/**$F_9NH(EO)_2NH_2$** interactions as monitored by static light scattering: (top) SLS data of *ss*DNA/**$F_9NH(EO)_2NH_2$** mixtures in buffer phosphate (NaCl 0.15 M, TRIS 0.05 M, pH 7.4) (left) *ss*DNA 10^{-7} M, (right) *ss*DNA 2×10^{-6} M, (bottom) schematic SLS representation of **$F_9NH(EO)_2NH_2$** binding *ss*DNA (left), schematic mechanism of *ss*DNA-fluorinated compound interactions (right): (a) the surfactant is in a monomeric form and *ss*DNA/**$F_9NH(EO)_2NH_2$** interactions are weak, (b) micellization of the surfactant on the *ss*DNA matrix occurs (c) maximum of monomers micellizing onto *ss*DNA, (d) demicellization and vesicle *ss*DNA-loading (e) only *ss*DNA-loaded fluorinated vesicles and (f) mixture of empty and *ss*DNA-loaded fluorinated vesicles.

increased, there is a reduction in the intensity of the diffused light. This might be due to concurrent demicellization of the surfactant from and formation of vesicles that encapsulate or externally bound *ss*DNA (d). Compared to the formation of micelles, formation of vesicles requires a significantly higher number of surfactant molecules, which are partly supplied from the exterior and partly provided from previously generated micelles. The scattered light intensity decrease observed at this stage is possibly due to the faster rate of demicellization compared to the rate of formation of *ss*DNA-containing vesicles. The inflection between (c) and (d) corresponds to the critical aggregation concentration of the surfactant vesicles in the presence of *ss*DNA (CACvDNA). Another plateau is then reached (e), where all *ss*DNA is trapped by **$F_9NH(EO)_2NH_2$** fluorinated vesicles. Free surfactant molecules might exist in solution, but they do not interact with *ss*DNA. By further increasing the surfactant concentration, "empty" vesicle might be formed (f); the final inflection point between (e) and (f) corresponds to the critical aggregation of surfactant vesicles (CACv).

Finally, all CAC values were shifted toward higher values upon increase of [*ss*DNA] in the initial solution (Table 2 and Fig. 5, top-right *vs.* top-left). This can be seen as a direct consequence of the larger number of molecular units involved in the initial aggregation of **$F_9NH(EO)_2NH_2$** on the *ss*DNA matrix (higher CACmDNA). Indeed, (a) curves in Fig. 5 are obtained with a limited number of data in the flat regions, (b) figures in Table 2 show that CACvDNA and CACv in the case of [*ss*DNA] = 2×10^{-6} M are 10 and 30 times CACmDNA, respectively, comparable to 10 and 50 times in the case of [*ss*DNA] = 10^{-7} M.

The binding of surfactant molecules to *ss*DNA was also investigated by ethidium bromide (EB) displacement with a premixed solution of *ss*DNA and EB. EB is a widely used cationic dye intercalating into DNA [44]. The ethidium ion displays a dramatic increase in fluorescence efficiency when it intercalates into DNA and a decrease of the fluorescence signal while the dissociation of EB from EB-DNA complexes occurs. By observing the changes in the fluorescence intensity of EB, it is possible to follow the DNA-surfactant interaction. Fig. 6 shows the fluorimetric titration of different *ss*DNA/EB complex solutions. For each solution, [EB] is 23 times higher than [*ss*DNA] (1 EB per nucleic base).

Two fluorescence profiles were observed depending on the *ss*DNA concentration. (i) At low [*ss*DNA] (0.1 and 0.3 μM, respectively), the surfactant concentration is below the CAC, as it was determined by SLS in buffer solution (0.01 mM). The fluorescence intensity decreases to a plateau which represents 55–65% of the maximum intensity. In these two cases, the saturation is reached for a ratio Z_+/Z_- of approximately 3. At low [**$F_9NH(EO)_2NH_2$**] ($Z_+/Z_- < 1$), the fluorescence intensity decreases, and the diminution is more important and faster as the [*ss*DNA] is increasing. This small variation is salt dependent [45–47]. With strong salt concentration, EB is not able to completely dissociate, which explains the aggregation of *ss*DNA/**$F_9NH(EO)_2NH_2$** complex before

Table 2
CAC of **$F_9NH(EO)_2NH_2$**/*ss*DNA mixtures in buffer phosphate as determined by SLS measurements.

	CAC_{mDNA} ($mol\,L^{-1}$)	CAC_{vDNA} ($mol\,L^{-1}$)	CAC_v ($mol\,L^{-1}$)
*ss*DNA (10^{-7} M)	10^{-6}	10^{-5}	$5{\cdot}10^{-5}$
*ss*DNA (2×10^{-6} M)	2×10^{-5}	2×10^{-4}	6×10^{-4}

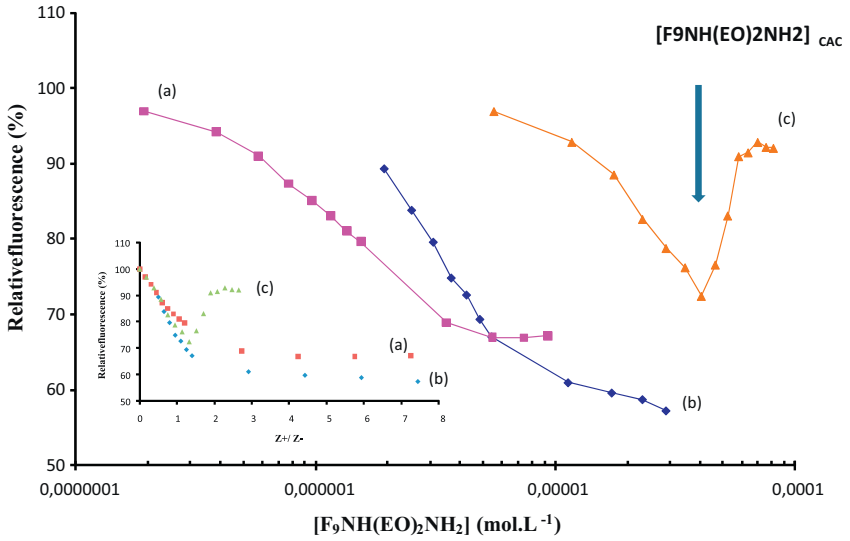

Fig. 6. Assay of EB displacement by **$F_9NH(EO)_2NH_2$**. The inset represents the variation of the relative fluorescence as a function of Z_+/Z_-. Z_+/Z_- is the ratio between positive, monocharged surfactant and negative, PO_4^--*ss*DNA charges. Each point is expressed as a percentage of the maximum fluorescence obtained with naked *ss*DNA (a) 0.1 μM *ss*DNA, 2.5 μM EB; (b) 0.3 μM *ss*DNA, 7 μM EB; (c) 2.5 μM *ss*DNA, 60 μM EB.

the total displacement of EB. (ii) For the strongest [*ss*DNA], 2.5 μM, one observes first a reduction then an increase in the relative fluorescence intensity before reaching a plateau at 90% of the maximum intensity for a ratio Z_+/Z_- of 2. For this *ss*DNA concentration, the CAC of the surfactant is quickly reached and the formation of aggregates or vesicles occurs before the total displacement of EB. The formation of aggregates is accompanied by a reformation of *ss*DNA/EB complexes and thus by an increase in the relative fluorescence intensity. Once the vesicles are formed, EB is not longer displaced indicating thus that the fluorinated amphiphile is not micellizing through electrostatic interactions onto *ss*DNA.

CD measurements are also widely used to determine conformational changes of *ss*DNA upon binding with surfactants. Absorbance and circular dichroism experiments were carried out on free *ss*DNA to find the wavelength with the maximum of absorbance (260 nm, see Fig. 1 in supporting information) and the optimal *ss*DNA concentration (2×10^{-6} M) for a sufficient dichroic signal (Fig. 7). Generally, the typical CD spectrum of a B-form [48–50] is characterized by a positive band centered on 278 nm, a negative band near 245 nm and a crossover point at *ca.* 260 nm (maximum wavelength in the UV spectrum); the A-form is characterized by a positive band centered on 260 nm, a negative band near 210 nm and the Z-form is characterized by a positive band centered on 260 nm, a negative band near 290 nm. CD spectra of our *ss*DNA exhibits a positive band near 278 nm and a negative band near 249 nm as shown in Fig. 7, indicating a helical structure similar to a B-form.

Variations in the 200–300 nm region of CD spectra upon addition of $F_9NH(EO)_2NH_2$ (Fig. 8) can be interpreted in terms of changes in DNA secondary structure. In particular, the intensities of the positive and negative bands were significantly affected by the presence of **$F_9NH(EO)_2NH_2$**: a positive minimum for $Z_+/Z_- = 3$ and a negative maximum for $Z_+/Z_- = 4$ were observed. The region between 200 and 300 nm can be interpreted in terms of changes in DNA secondary structure. This spectrum (Fig. 8) shows a significant variation of the intensity of the positive and negative bands with a positive minimum for $Z_+/Z_- = 3$ and a negative maximum for $Z_+/Z_- = 4$. For $Z_+/Z_- < 6$, the reduction in intensity of CD band at 275 nm can be due to *ss*DNA aggregation through electrostatic interactions, whereas for $Z_+/Z_- > 8$ the intensity of the CD band increases to even higher values than the native *ss*DNA, which could be due to the *ss*DNA confinement into the core of the vesicles. Moreover, as shown in Fig. 8 and further evidenced in Fig. 9, the crossing point between negative and positive Cotton effect is right-shifted from 258 nm to 263 nm with the increase in surfactant concentration until $Z_+/Z_- = 4$. Further increase in the surfactant concentration is accompanied by a left-shift to 257 nm. This shows a strong interaction with the single strain of the *ss*DNA

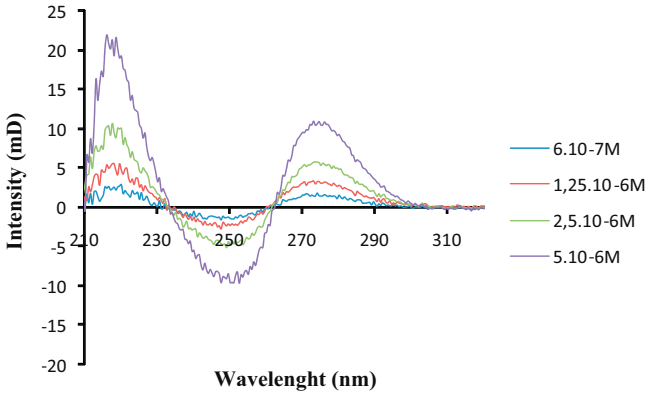

Fig. 7. CD spectra for [*ss*DNA] = 2 μM at different concentrations of surfactant.

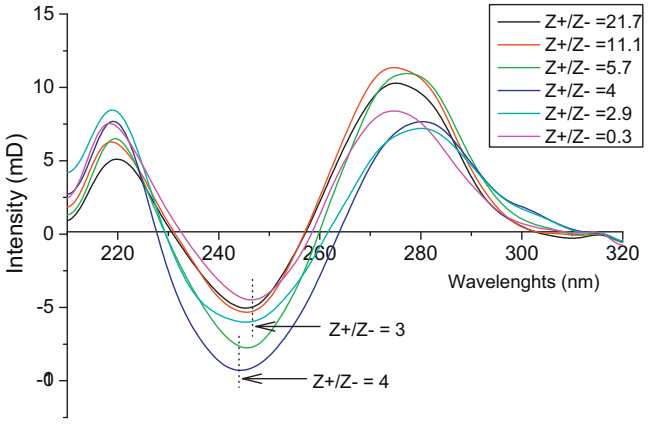

Fig. 8. CD spectra of 2 μM *ss*DNA in the presence of various concentrations of **$F_9NH(EO)_2NH_2$**.

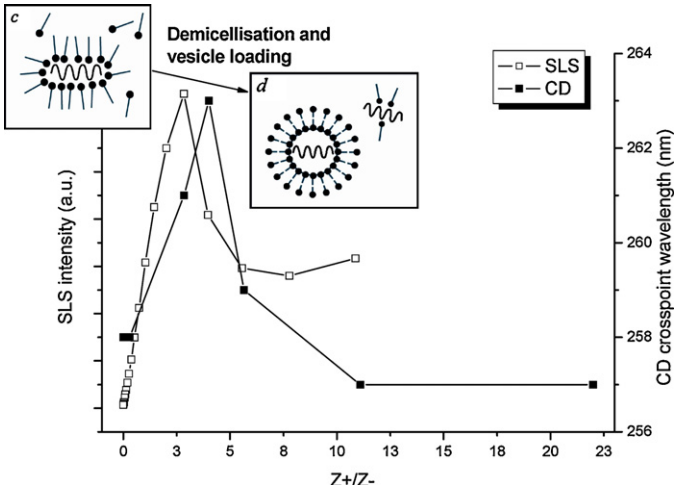

Fig. 9. Dependence of SLS intensity and CD crosspoint wavelength on the $F_9NH(EO)_2NH_2$/DNA molar ratio.

accompanied by a destructuration of the *ss*DNA helix and stacking of the bases. This might indicate that either the *ss*DNA undergoes a transition from B-form to a less organized, random like-polymer, phase or that the *ss*DNA is uploaded into vesicles. The last hypothesis seems to be confirmed by the results obtained in SLS measurements, where the decrease in scattered light was explained by the demicellization of the compound and spontaneous *ss*DNA-vesicle formation. The results of SLS and CD experiments are in good agreement, and that both techniques point to a transition micelles to vesicles occurring at Z_+/Z_- 3–4 (Fig. 9).

3.3. Toxicity studies

Another goal of this study was to determine the cytotoxicity of fluorinated surfactant $F_9NH(EO)_2NH_2$ as compared to commercially available non-viral vectors, IC_{50} values of which are in the μM range. We decided to report here a preliminary toxicity study of $F_9NH(EO)_2NH_2$ because this parameter is considered of primary importance in a first step to appreciate the validity of our approach in the development of potent new drug vectors. The toxicity of $F_9NH(EO)_2NH_2$ was estimated in an *in vitro* assay by measuring cellular viability in the presence of increasing amounts of $F_9NH(EO)_2NH_2$. It was found that MRC-5 cell viability was weakly affected, as shown by the viability evolution during the time course of experiments of MRC-5 cells treated with $F_9NH(EO)_2NH_2$ (Fig. 10). The cell viability was assessed after 1, 2 and 7 days of incubation.

The determined IC_{50} values are comparable to those of commercially available non-viral vectors and remain constant in time (*i.e.* 5.3×10^{-5} M, 5×10^{-5} M, 4.6×10^{-5} M; at 24, 48 and 168 h, respectively).

Cell viability data indicate that fluorocarbon $F_9NH(EO)_2NH_2$ is not toxic on human cells below 40 μM, which means that above the CAC value these fluorinated vesicles could be used in vector-mediated biological applications.

4. Conclusions

We have reported in the present work the synthesis of novel monocatenar fluorinated surfactant bearing a diamino-diethoxylated head group. This amphiphile was design in order to respond to three criteria: (i) *a fluorinated hydrophobic tag* responsible of self-assembling and suited for spontaneous-vesicle-formation, (ii) *an ethylene oxide moiety* sufficiently hydrophilic so that the compound could be soluble at high concentration, up to 1 mM, and avoiding thus precipitation of the surfactant–*ss*DNA complex and (iii) *a protonated* at physiological pH *primary amine* responsible of binding. Thus, the *ss*DNA-fluorous surfactant interaction is made through electrostatic interactions between the external primary amine and the phosphate groups. By externalizing the binding site, the repulsions between the bulky ethylene oxide moiety and the anionic *ss*DNA could be avoided, whereas the flexibility of the polar head allowed conformational changes for an optimum complexation. At low surfactant concentration (lowest then the CAC of the fluorous surfactant) only micellization occurs, in agreement with the classical behavior of *ss*DNA-cationic surfactant interactions, up to a certain value where *ss*DNA-vesicles are formed. In other terms, above CAC reorganization of the *ss*DNA-surfactant complex might take place, probably due to the spontaneous vesicle formation properties of the fluorinated surfactant.

In this study we show an original design of a monocharged cationic surfactant able the efficiently complex *ss*DNA in a unique

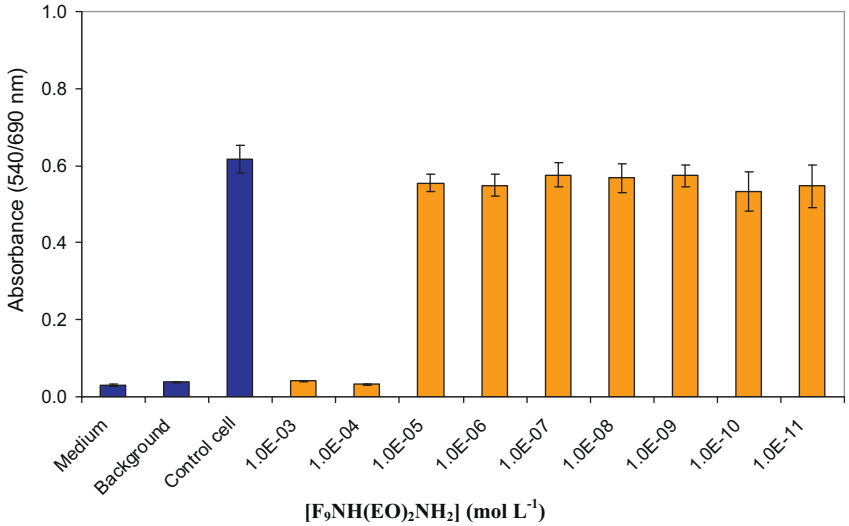

Fig. 10. MTT assay performed with $F_9NH(EO)_2NH_2$ on MRC-5. Histograms were typical of three independent experiments at 168 h. Medium: MEM alone. Background: MEM with drug. Control cells: untreated.

way. This represents a straightforward approach for oligonucleotide vectors, in which *ss*DNA is confined into aqueous core of the vesicles and slightly stabilized through electrostatic interaction between the positively charged vesicle surface and negatively charged *ss*DNA. The presence of fluorocarbon chain allows the formation of spontaneous vesicles, and thus for a relatively short, only nine carbons chain length, with respect to their hydrogenated homologues.

Moreover, the combination of the spontaneously formed vesicle properties, oligonucleotide complexation and the non-toxicity of the fluorinated surfactant demonstrate the great potential of these amphiphiles for biomedical applications such as gene therapy or RNA interference.

Acknowledgments

ND thanks the French Ministry of further Education and Research for his PhD grant. Authors thank J. Ghanbaja for TEM micrographs.

Appendix A

Supporting information available: (1) UV–Vis spectra of *ss*DNA at different concentrations. This material is available free of charge via the Internet at http://pubs.acs.org.

References

[1] M.A. Mintzer, E.E. Simanek, Chem. Rev. 109 (2009) 259–302.
[2] L. De Laporte, J. Cruz Rea, L.D. Shea, Biomaterials 27 (2006) 947–954.
[3] S. Bhattacharya, A. Bajaj, Curr. Opin. Chem. Biol. 9 (2005) 647–655.
[4] P. Barthélémy, S.J. Lee, M. Grinstaff, Pure Appl. Chem. 77 (2005) 2133–2148.
[5] K. Gao, L. Huang, Mol. Pharmacol. 6 (2009) 651–658.
[6] Y. Xu, F.C. Szoka, Biochemistry 35 (1996) 5616–5623.
[7] S. Bhattacharya, S.S. Mandal, Biochim. Biophys. Acta: Biomembr. 1323 (1997) 29–44.
[8] S. Bhattacharya, S.S. Mandal, Biochemistry 37 (1998) 7764–7777.
[9] D. Simberg, D. Hirsch-Lerner, R. Nissim, Y. Barenholz, J. Liposome Res. 10 (2000) 1–13.
[10] C. Nicolazzi, M. Garinot, N. Mignet, D. Scherman, M. Bessodes, Curr. Med. Chem. 10 (2003) 1263–1277.
[11] B. Martin, M. Sainlos, A. Aissaoui, N. Oudrhiri, M. Hauchecorne, J.-P. Vigneron, J.-M. Lehn, P. Lehn, Curr. Pharm. Des. 11 (2005) 375–394.
[12] T. Montier, T. Benvegnu, P.-A. Jaffrès, J.-J. Yaouanc, P. Lehn, Curr. Gene Ther. 8 (2008) 296–312.
[13] M. Morille, C. Passirani, A. Vonarbourg, A. Clavreul, J.-P. Benoit, Biomaterials 29 (2008) 3477–3496.
[14] S. Bhattacharya, A. Bajaj, Chem. Commun. (2009) 4632–4656.
[15] D. Zhi, S. Zhang, B. Wang, Y. Zhao, B. Yang, S. Yu, Bioconjug. Chem. 21 (2010) 563–577.
[16] E. Klein, C. Leborgne, M. Ciobanu, J. Klein, B. Frisch, F. Pons, G. Zuber, D. Scherman, A. Kichler, L. Lebeau, Biomaterials 31 (2010) 4781–4788.
[17] J. Gaucheron, C. Santaella, P. Vierling, Bioconjug. Chem. 12 (2001) 569–575.
[18] P. Vierling, C. Santaella, J. Greiner, J. Fluorine Chem. 107 (2001) 337–354.
[19] J. Gaucheron, C. Santaella, P. Vierling, Bioconjug. Chem. 12 (2001) 114–128.
[20] J. Gaucheron, C. Boulanger, C. Santaella, N. Sbirrazzuoli, O. Boussif, P. Vierling, Bioconjug. Chem. 12 (2001) 949–963.
[21] C. Boulanger, C. Di Giorgio, J. Gaucheron, P. Vierling, Bioconjug. Chem. 15 (2004) 901–908.
[22] K. Fabio, C. Di Giorgio, P. Vierling, Biochim. Biophys. Acta 1724 (2005) 203–214.
[23] L. Le Gourriérec, C. Di Giorgio, J. Greiner, P. Vierling, New J. Chem. 32 (2008) 2027–2042.
[24] S. Denoyelle, A. Polidori, M. Brunelle, P.Y. Vuillaume, S. Laurent, Y. ElAshari, B. Pucci, New J. Chem. 30 (2006) 629–646.
[25] E. Klein, M. Ciobanu, J. Klein, V. Machi, T. Vandamme, C. Leborgne, B. Frisch, F. Pons, A. Kichler, G. Zuber, L. Lebeau, Bioconjug. Chem. 21 (2010) 360–371.
[26] N. Dupuy, A. Pasc, F. Baros, C. Gérardin, J. Fluorine Chem. 132 (2011) 892–897.
[27] T.J. Mosmann, Immunol. Methods 65 (1983) 55–63.
[28] S. Fontanay, M. Grare, J. Mayer, C. Finance, R.E. Duval, J. Ethnopharmacol. 120 (2008) 272–276.
[29] S. Achilefu, L. Mansuy, C. Selve, S. Thiébaut, J. Fluorine Chem. 70 (1995) 19–26.
[30] S. Thiebaut, C. Gérardin, J. Amos, C. Selve, J. Fluorine Chem. 73 (1995) 179–184.
[31] S. Thiébaut, C. Gérardin-Charbonnier, C. Selve, J. Fluorine Chem. 82 (1997) 131–138.
[32] S. Cosgun, C. Gérardin-Charbonnier, J. Amos, C. Selve, J. Fluorine Chem. 125 (2004) 55–61.
[33] N. Dupuy, A., Pasc, E., Mayot, S., Cosgun, C. Gérardin-Charbonnier, J. Fluorine Chem., in press.
[34] O. Pornsunthorntawee, S. Chavadej, R. Rujiravanit, Colloids Surf. B 72 (2009) 6–15.
[35] A.Pasc-Banu, M. Blanzat, M. Belloni, E. Perez, C. Mingotaud, I.Rico-Lattes, T. Labrot, R. Oda, J. Fluorine Chem. 126 (2005) 33–38.
[36] J.G. Riess, J. Drug Target. 2 (1994) 455–468.
[37] M.-P. Krafft, J.G. Riess, Biochimie 80 (1998) 489–514.
[38] J.G. Riess, Tetrahedron 58 (2002) 4113–4131.
[39] M.-P. Krafft, F. Giulieri, J.G. Riess, Angew. Chem. Int. Ed. Engl. 32 (1993) 741–743.
[40] J. Pencer, F.R. Hallett, Langmuir 19 (2003) 7488–7497.
[41] T. Blessing, J.-S. Remy, J.-P. Behr, Proc. Natl. Acad. Sci. U. S. A. 95 (1998) 1427–1431.
[42] E. Dauty, J.-S. Remy, T. Blessing, J.-P. Behr, J. Am. Chem. Soc. 123 (2001) 9227–9234.
[43] C. Chittimalla, L. Zammut-Italiano, G. Zuber, J.-P. Behr, J. Am. Chem. Soc. 127 (2005) 11436–11441.
[44] V.A. Izumrudov, M.V. Zhiryakova, A.A. Goulko, Langmuir 18 (2002) 10348–10356.
[45] H.S. Basu, H.C.A. Schwietert, B.G. Feuerstein, L.J. Marton, Biochem. J. 269 (1990) 329–334.
[46] A.J. Geall, I.S. Blagbrough, J. Pharm. Biomed. Anal. 22 (2000) 849–859.
[47] T.I. Tikchonenko, S.E. Glushakova, O.S. Kislina, N.A. Grodnitskaya, A.A. Manykin, B.S. Naroditsky, Gene 63 (1988) 321–330.
[48] J.C. Wang, Proc. Natl. Acad. Sci. U. S. A. 76 (1979) 200–203.
[49] C.A. Sprecher, W.A. Baase, W.C. Jonson Jr., Biopolymers 18 (1979) 1009–1019.
[50] J. Kypr, I. Kejnovska, D. Renciuk, M. Vorlickova, Nucleic Acids Res. 37 (2009) 1713–1725.